Dynamics of Active Magnetic Thrust Bearings*

Satoru FUKATA**, Yoshinori KOUYA***,
Takashi SHIMOMACHI****,
Yutaka MIZUMACHI***** and Makoto KUGA******

A linear model considering the effect of eddy currents is shown to be useful for the analysis of the dynamics of active magnetic thrust bearings in which electromagnet cores are composed of solid steel. The dynamics of the magnetic control force are modeled by the first-order time-lag system with unknown parameters: gain and time constant. The parameters are estimated from experimental results that indicate the static relation between the coil current and the magnetic control force, and the frequency response of magnetic flux for an input signal to a power amplifier. The effect of eddy currents on the dynamics is confirmed by the frequency characteristics of magnetic flux for the coil current. Model simulations with estimated parameters are compared with experimental results, and good agreement is obtained in frequency response in a linear range and in impulse responses with rotor displacements smaller than half the air gap.

Key Words: Mechatronics, Automatic Control, Dynamics of Machinery, Magnetic Bearing, Modeling

1. Introduction

In active magnetic bearings which support a rotor with no contact by electromagnetic forces controlled through coil currents, the characteristics of the electromagnets determine the performance of the bearings. Magnet cores of laminated stacks are applied to the radial bearings in practical use. To the thrust bearings, however, solid cores are applied in most cases mainly because of their construction. If the effect of eddy currents in the cores is not negligible, it delays the generation of the magnetic flux (i.e., the control force), whereas the magnetic brakes for the rotation of a rotor might be negligible. This delay may lead to a poor performance of the rotor-displacement control.

The dynamics of the radial bearings has been analyzed theoretically and experimentally in a number of papers, for example, Refs. (1)～(3) and their references. For the thrust bearings, a few papers have been published with only experimental results[4], and with numerical and experimental results[5]. The analysis of the dynamics of the thrust bearings might be much more difficult than that of the radial bearings, because of the effects of eddy currents and the effect of the hysteresis of magnetic force.

A unified linear model, which considers the time lag of the magnetic force due to the eddy currents and is applicable to both the radial and thrust bearings, was presented in Ref. (3) in application to the radial bearings. This unified model, however, did not clearly illustrate its usefulness as a result of its application to the case of laminated cores. The purpose of this paper is to show the effectiveness of this unified model with

* Received 21st December, 1990. Paper No. 89-0680B.
** Department of Mechanical Engineering, Kyushu University, 6-10-1 Hakozaki, Higashi-ku, Fukuoka 812, Japan
*** Faculty of Education, Saga University, 1 Honjyo-machi, Saga 840, Japan
**** Nagasaki University, 1-14 Bunkyo-machi, Nagasaki 852, Japan
***** Matsuura Power Station, Kyushu Power Electric Inc., 166 Shirahamamen Shisa-machi, Matsuura, Nagasaki Pref. 859-45, Japan
****** Nagasaki Research & Development Center, Mitsubishi Heavy Industries Ltd., 5-717-1 Fukahori-machi, Nagasaki 851-03, Japan

application to the thrust bearing, in which the effect of eddy currents is not negligible. The characteristics of the electromagnets with solid steel cores are examined for the effect of eddy currents on the generation of magnetic flux, and for the hysteresis of magnetic flux to check the effectiveness of linearity. The dynamic characteristics of the control force are approximated by a first-order time-lag system in which the time constant is estimated from an experimental result. Model simulations are compared with experimental results in frequency and impulse responses.

2. Modeling of Active Magnetic Bearings

Figure 1 illustrates the structure of active magnetic thrust bearings in which the poles of electromagnets are concentric circles. A rotor is initially attracted by the bias forces of the magnets. The position of the rotor is regulated by a differential force generated by the pair of magnets through control of the two coil currents. The control signals which have different signs, plus or minus, are introduced into the two power amplifiers; their absolute values may be the same. We assume that the characteristics of the two electromagnet systems are the same.

The equation of rotor motion is represented by

$$m\ddot{x}=f+d, \tag{1}$$

where

m : mass of rotor
x : displacement of rotor
f : control force
d : disturbance force.

2.1 Dynamics of magnetic force

We assume that there is no leakage and no overflow of magnetic flux in magnetic circuits, and that the magnetic resistance in the magnet cores is negligible compared with that in the air gap. We also suppose that the inclination of the rotor is small.

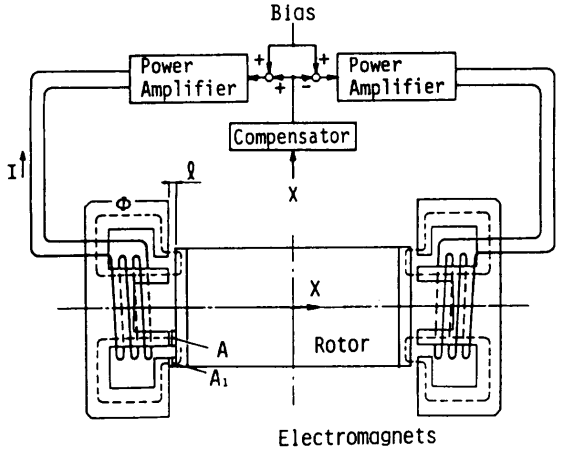

Fig. 1 Structure of active magnetic thrust bearings

First we consider a single electromagnet system. The following notations are used

E_1 : input voltage to magnet coil
R : resistance of magnet coil
I : coil current
N : turns of coil
Φ : magnetic flux
R_e : equivalent resistance for eddy currents
I_e : equivalent eddy current in magnet core
R_m : resistance of magnetic circuit
l : air-gap length
μ_0 : permeance of air, $4\pi\times10^{-7}$ H/m
A, A_1 : area of magnet poles

In addition, the subscript 0 in the variables denotes the value of a steady state.

From the relation in the magnet coil, we obtain the equation

$$E_1=RI+N\dot{\Phi}. \tag{2}$$

We neglect the skin effect of magnetic flux in the cores and simplify the complex circuits of eddy currents in the cores to a one-loop circuit which is equivalent to the effects of the combined eddy currents[6]. Under this simplification, for the useful magnetic circuit, we obtain the following relation:

$$NI+I_e=R_m\Phi, \tag{3}$$

where the resistance of the magnetic circuit, R_m, may be given by[7]

$$R_m=\frac{l}{\mu_0 A}+\frac{l}{\mu_0 A_1}. \tag{4}$$

For the electric circuit of the assumed single eddy current loop, a relation similar to Eq.(2) is

$$0=R_eI_e+\dot{\Phi}. \tag{5}$$

The magnetic-attractive force is expressed as[7]

$$F=\frac{\Phi^2}{2\mu_0 A}+\frac{\Phi^2}{2\mu_0 A_1}. \tag{6}$$

We consider power amplifiers with current control. If the control law is a proportional-integral (PI) action, then the output voltage of the power amplifier (input voltage to the coil) may be represented by

$$E_1=p[(bE-I)+gz],$$
$$\dot{z}=bE-I, \tag{7}$$

where

E : input voltage to power amplifier
b : gain of power amplifier
p : gain of proportional action
g : gain of integral action.

For convenience, we define a variable Q by

$$Q=\frac{R_{m0}}{N}\Phi. \tag{8}$$

This variable has the same unit as current, the same characteristics as the flux in dynamics, and the same value as the coil current in statics. Eliminating E_1, I, I_e and z from the above equations, and replacing Φ by Q, we obtain the following relation:

$$kT\ddot{Q}+\left(k\frac{l}{l_0}+k_e\right)\dot{Q}+\left(k\frac{\dot{l}}{l_0}+\frac{l}{l_0}\right)Q=b(T_c\dot{E}+E), \tag{9}$$

where

$$T=\frac{1}{R_{m0}}\left(\frac{N^2}{R'}+\frac{1}{R_e}\right),\ k=\frac{R'}{pg},\ k_e=\frac{1}{R_{m0}R_e},\ T_c=\frac{1}{g},$$
$$R'=R+p. \tag{10}$$

In this case, the magnetic force, Eq.(6), is written as

$$F=\frac{\mu_0 AN^2}{2(1+a)}\left(\frac{Q}{l_0}\right)^2,\ a=\frac{A}{A_1}. \tag{11}$$

Now, we consider deviations from a steady state:

$$Q=I_0+q,\ l=l_0+x,\ E=E_0+e. \tag{12}$$

Then, Eq.(9) is written as

$$kT\ddot{q}+\left(k+k\frac{x}{l_0}+k_e\right)\dot{q}+\left[1+\frac{x}{l_0}+k\frac{\dot{x}}{l_0}\right]q$$
$$+I_0\left(\frac{x}{l_0}+k\frac{\dot{x}}{l_0}\right)=b(T_c\dot{e}+e). \tag{13}$$

The increment of the magnetic force, f, is represented by

$$f=2\frac{F_0}{I_0}\left(q+\frac{q^2}{I_0}\right). \tag{14}$$

Thus, the dynamics of the incremental magnetic force are modeled by Eqs.(13) and (14) for the single electromagnet system.

Incidentally, if we take $g\to 0$ in Eq.(9), i.e., a proportional action in the current control, then we have the simpler form

$$T\dot{Q}+\frac{l}{l_0}Q=b\frac{p}{R'}E. \tag{15}$$

In the above model, Eq.(13) or (15), the effects of eddy currents are in the resistance R_e. For the magnet cores of laminated stacks, this resistance is large, and so the effect of eddy currents is small. The feedback control of the coil current compensates for the lag of the flux generation for the magnet coil, but does not do so for the effect of the eddy currents. The time lag caused by eddy currents becomes relatively small when compared with the lag due to the magnet coil if we take a large coil turn and/or a small control gain in the current control.

In addition, it is difficult to derive a simple expression of the coil current similar to the example above. If the air gap is constant, then we can obtain a simple relation between the flux (Q) and the coil current (I) which shows that the generation of the flux is related to the coil current by the first-order time-lag system with the time constant of $1/R_e$[3].

2.2 Dynamics of control force

The dynamics of the incremental magnetic force were modeled by Eqs.(13) and (14) for each of a pair of electromagnet systems. We will mark the variables of the magnet systems with the subscript 1 for the side from which the rotor parts when the rotor moves in the positive direction (the left side in Fig. 1), and with the subscript 2 for the other side (the right side in Fig. 1). Applying Eq.(14) to the pair of magnets, we have the net increment of the force,

$$f=2\frac{F_{10}}{I_{10}}\left[\left(\frac{I_{20}}{I_{10}}q_2-q_1\right)+\frac{1}{2I_{10}}(q_2^2-q_1^2)\right]. \tag{16}$$

Neglecting the second-order terms results in

$$f=K_F q, \tag{17}$$

where

$$K_F=4\frac{F_{10}}{I_{10}} \tag{18}$$

$$2q=\frac{I_{20}}{I_{10}}q_2-q_1. \tag{19}$$

In a similar way, we obtain the linearized equation of Eq.(13) as follows:

$$kT\ddot{q}+(k+k_e)\dot{q}+q-a_l(x+k\dot{x})=b(T_c\dot{e}+e), \tag{20}$$

where

$$a_l=\frac{I_{10}}{2l_0}\left[1+\left(\frac{I_{20}}{I_{10}}\right)^2\right] \tag{21}$$

$$e=\frac{1}{2}\left(\frac{I_{20}}{I_{10}}e_2-e_1\right). \tag{22}$$

To derive a simpler model, we can approximate Eq. (20) by the following first-order equation:

$$T'\dot{q}+q-a_l(x+k\dot{x})=be. \tag{23}$$

Thus, we have the linearized model of Eqs.(1), (17) and (23) for the thrust bearings. Equation (23) differs from a model derived for the proportional current control[3] only in the term with the velocity added to the flux change due to the displacement.

The purpose of adding the integral action to the current control is to ensure the linearity between the input voltage and the output coil current of the power amplifiers, and to compensate for the dependence of the coil current on the temperature caused by the variation of the coil resistance, although this dependence was small.

If we adopt power amplifiers with only a proportional control, then we have a simpler model with $T'=T$ and $k=0$ in Eq.(23). The proportional action plays a role not only in reducing the time lag, but also in compensating both the nonlinearity of the input-output relation of power amplifiers and the dependence of the coil current on the temperature. It is desirable, therefore, to make the proportional gain as large as possible.

2.3 Control system

As a compensator of the analog control of the rotor displacement, we utilize a proportional-integral-derivative (PID) action whose transfer function is given by the Laplace transform

$$C(s)=K_P+\frac{K_I}{1+T_I s}+\frac{K_D s}{1+T_D s}, \tag{24}$$

where K_P, K_I and K_D are gains, and T_I and T_D are time constants. The block diagram of the control system is shown in Fig. 2, where

$R_0(s)$: reference input

$U(s)$: control input
$U_0(s)$: disturbance input
$D(s)$: disturbance force
$Y(s)$: output of displacement sensor
K_y : gain of displacement sensor.

3. Characteristics of Magnetic Force

Figure 3 shows the mechanical part of the experimental setup with the two radial bearings and the thrust bearing. The thrust bearing located at the end of the rotor is composed of stator parts ⑤ and rotor parts ⑥ of electromagnets made of solid steel, and a displacement sensor of eddy current type ⑦. A sensor target made of aluminum is installed in the center of the rotor end. The magnet cores of the thrust bearing are shown in Fig. 4. The main data of the thrust bearing are reported in Table 1. The radial bearings

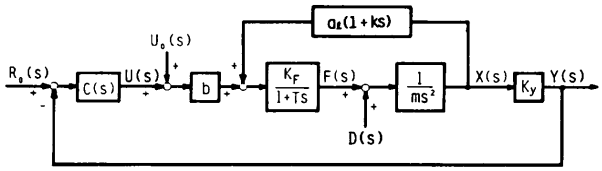

Fig. 2 Block diagram of linear model

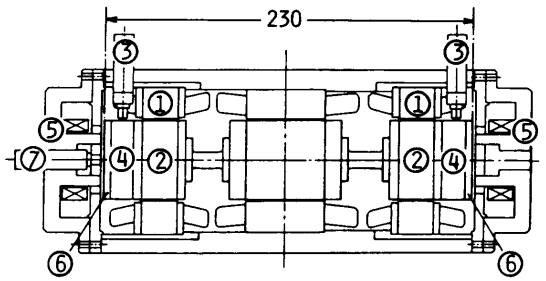

Fig. 3 Experimental setup

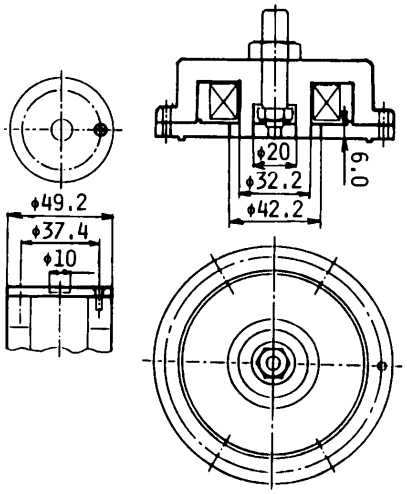

Fig. 4 Magnet cores of thrust bearing
left : rotor, right : stator

are composed of stators ①, rotors ②, and displacement sensors ③ with their target rings ④.

We used chopper amplifiers (carrier frequency 15 kHz) with a pulse-width-modulated PI control. The setup was placed so as not to be affected by gravity, i. e., no load for the thrust bearing in the steady state, and the control input signals to the two power amplifiers were represented by the same absolute value. The parameters of the PID compensator were selected as shown in Table 1.

3.1 Static characteristics

The parameters b and T_c are estimated to be $b=0.60$ A/V and $T_c=3.1$ ms from the electric circuits of the current controller of the power amplifiers (b is also estimated by the same value from the input-output relation in steady states). The gain p was estimated as follows: only for the proportional control the gradient of the output current for the input voltage is given by $I/E=bp/R'$ from Eq.(15) in steady states; the experimental results determined this value as 0.56 A/V, from which it follows that $p\simeq 17$. From these values, we obtain the parameter $k=3.3$ ms in Eq.(10).

We measured the force constant K_F of the thrust bearing in the steady states where the bearings are all in action. The rotor was loaded by a spring balance (a pulling force) attached to the end of the rotor on the opposite side of the displacement sensor. Before the measurement, we loaded the rotor in the opposite direction of the spring force with a bar with a force

Mass of Rotor	$m=2.3$	kg
Coil: Number of turns	$N=200$	
Resistance (at 21℃)	$R=1.2$	Ω
Inductance	$L=16\times10^{-3}$	H
Area of magnet pole	$A=5.0\times10^{-4}$	m²
	$A_1=5.1\times10^{-4}$	m²
Gap length	$\ell_0=0.8\times10^{-3}$	m
Power Amplifier Gain:	$b=0.60$	A/V
Constants:	$T_c=3.1\times10^{-3}$	s
	$k=3.3\times10^{-3}$	s
Gain of displacement sensor	$K_y=25.5\times10^3$	V/m
Bias current	$I_0=2.0$	A
Force constant	$K_F=90$ (Experiment.)	N/A
	$=80$ (Theoret.)	
Time constant	$T'=1.4\times10^{-3}$	s
Gap constant	$Q_\ell=2.5\times10^3$	A/m
Parameters of compensator		
Time constants:	$T_I=1.1$	s
	$T_D=0.1\times10^{-3}$	s
Gains:	$K_P=0.55$	
	$K_I=51$	
	$K_D=2.5\times10^{-3}$	s

similar to the maximum force in the following measurements, so as to demonstrate the hysteresis of the control force. After release from the force, the coil currents were measured for increasing and decreasing spring forces.

The relationship between the spring force and the difference of the pair-coil currents is plotted as in Fig. 5. In Figs. 5 and 6 the percentages denote the ratios of the amplitude of the coil current variation for the bias current 2.0 A. As predicted, we see that the control force has hysteresis, and that the force constant varies from the variations of the coil current. The force constant defined by Eq.(18) is estimated by the ratio of the spring force for the change of the coil current, ΔI. This value may be given by an average gradient of 90 N/A and 100 N/A for the current variations of 25% and 50%, respectively. We determine this theoretical value as 80 N/A from Eq.(18) by neglecting the hysteresis.

Data below were obtained for the one-electromagnet system with the fixed air gap of 0.8 mm. Figure 6 shows the variations of the flux density measured with a gaussmeter on the outer pole in steady states. We confirm the hysteresis of the magnetic flux, and see that the hysteresis loop of the amplitude 25% is inscribed to that of 50%, and that the gradient of the line connecting the two terminals of the loop varies with the amplitudes, and its value for the amplitude 25% is about 95% of that of 50%.

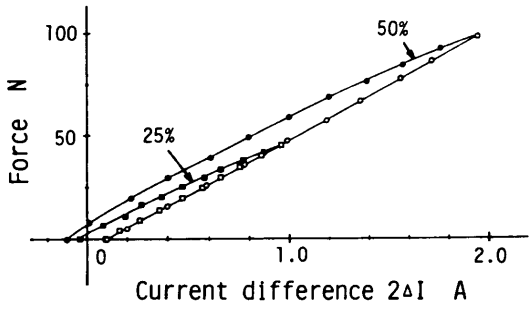

Fig. 5 Relationships between net force and coil current

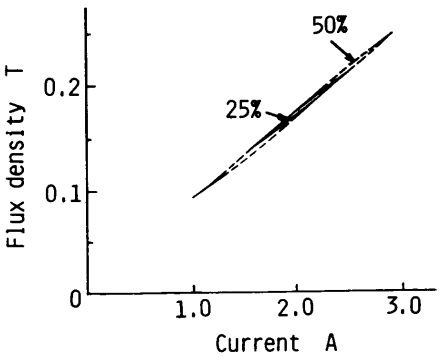

Fig. 6 Flux density for coil current

3.2 Dynamics

It is so difficult to estimate numerically the resistance for eddy currents, R_e, that it may be practical to obtain it from an experimental result. With our model, however, we need not determine the value itself, but only to obtain the time constant T' that includes its effect.

Figure 7 shows the frequency characteristics of the flux density of the outer pole for the input signal into the power amplifier under the same conditions as in the preceding section. The percentages in the figures hereafter denote the ratios of the input amplitude for the bias input voltage 3.3 V corresponding to the bias current 2.0 A. The gains of the responses are shown by the values obtained directly from the measurements, so that the relative values are meaningful. We see that the gain and the phase shift vary from the input amplitudes. We may approximate the characteristics of the 25% amplitude by the first-order time-lag system with the time constant 1.4 ms from the fact that a frequency of about 115 Hz provides a phase shift of 45% degrees. The parameters obtained in this section are summarized in Table 1.

To prove the effect of eddy currents on the generation of the magnetic flux, we observed other responses in the previous measurements. Figure 8 shows the frequency responses of the coil current for the input signal, and Fig. 9 shows the characteristics

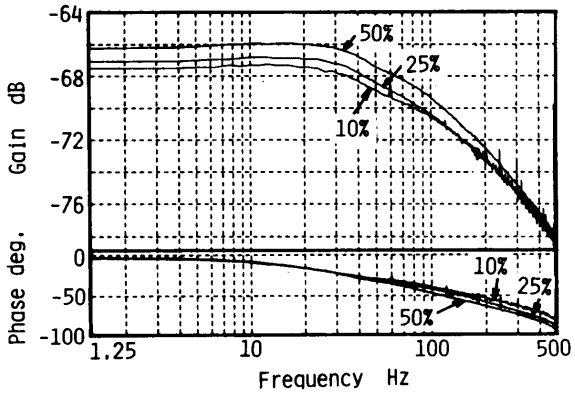

Fig. 7 Frequency responses of flux density

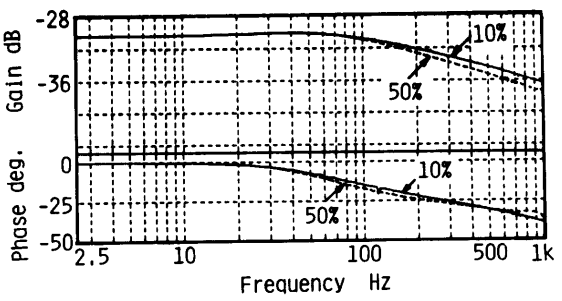

Fig. 8 Frequency responses of coil current

of the magnetic flux density for the coil current. We confirm that the generation of the magnetic flux is delayed more than that of the coil current.

4. Experiments and Simulations

The experimental data were obtained under the same conditions as in the previous section with no initial load. The rotor remained at rest (i. e., nonrotation) because the characteristics of the thrust bearing system are considered to be the same at rest and in rotation. The absolute value of the control signal (the output of the PID compensator) was restricted to about 3.3 V with zener diodes, so that the control coil current may be limited by the same value around the bias current 2.0 A.

The simulation data were obtained using the linear model realized with analog circuits, utilizing the same PID compensator (with limiters) that was used in the experiments.

4.1 Frequency responses

Instead of applying disturbance forces directly on the rotor, we applied magnetic forces by superimposing sinusoidal inputs on the control signal ($U_0(s)$ in Fig. 2). Figure 10 shows the frequency responses of the rotor displacement, but only the gain for the amplitude of 10%. The gains in the two cases are slightly different from each other around the frequency of 130 Hz: the gain of the amplitude of 20% is greater than that of 10%, and has a small rise. This difference may be due to the characteristics of the magnetic force which vary from the amplitudes of the control signal, as is shown in Fig. 7. The simulation result is represented by broken lines, which is closer to the experimental result in the case of 20%.

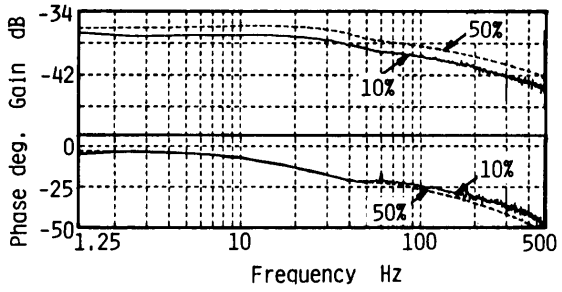

Fig. 9 Frequency characteristics of flux density for coil current

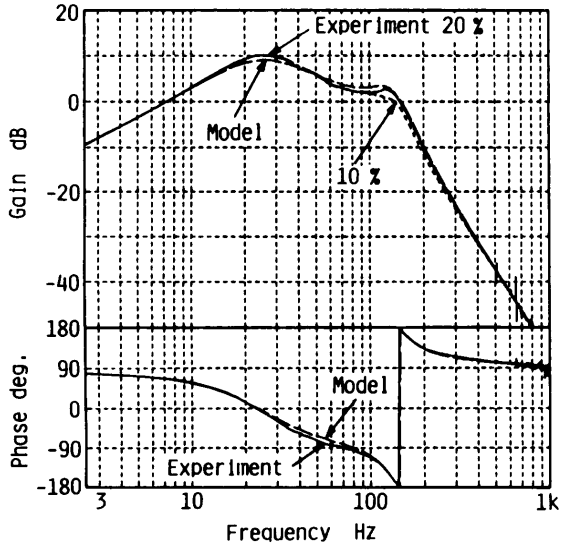

Fig. 10 Frequency responses of displacement for disturbance

4.2 Impulse responses

Motions of the rotor for impulses on the face of the rotor end were compared in the experiments and simulations. In the simulations, impulses generated with an analog circuit were input in the same position as the direct disturbance force, and their magnitudes were adjusted to show a maximum displacement similar to the experimental results. Figure 11 shows the results of two cases: the upper part represents a small displacement without saturation of the control signal, and the lower part illustrates a displacement of about 40% of the air gap with saturation of the

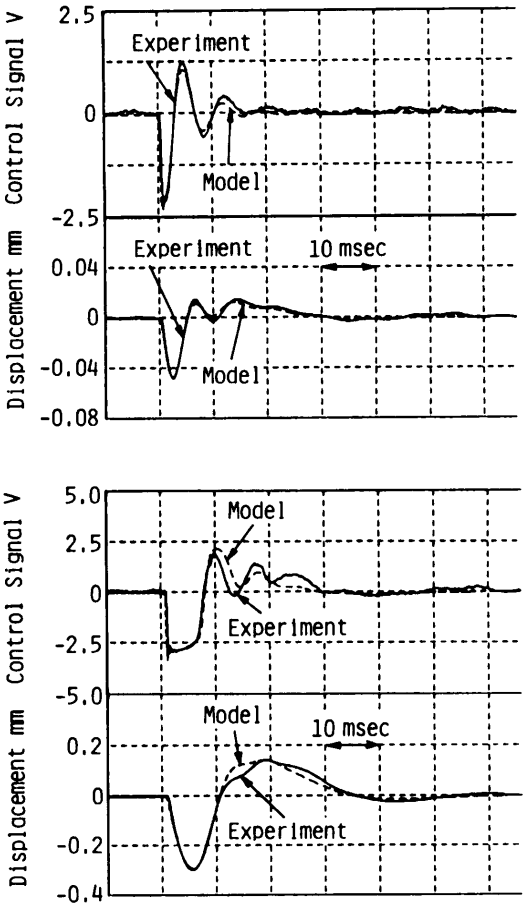

Fig. 11 Impulse responses

control signal. The simulation is good agreement with the experimental results.

5. Conclusions

The dynamics of an active magnetic thrust bearing, in which the magnet cores are made of solid steel, have been analyzed numerically and experimentally. First, to obtain the model parameters, the characteristics of the electromagnets were examined for the effects of eddy currents in the magnet cores in dynamics and for the hysteresis of the magnetic force in statics. Next, in the case of frequency responses and impulse responses of the rotor motion, simulations by the linear model have been compared with the experimental results for relatively small deviations of the displacement. The results showed the usefulness of the presented linear model.

Here we did not need to estimate the equivalent resistance for an eddy current itself, because we needed only to have the time constant that includes this resistance, and which we obtained from an experimental result. It might be necessary to develop a method for estimating this resistance beforehand to utilize it in the design stage.

We analyzed the effects of eddy currents only on the time lag of the magnetic force ; however, the eddy currents also affect the magnitude of the magnetic force in dynamics as a result of the skin effect of magnetic flux. Hence, it is necessary to consider this effect in general, especially in its application in higher frequencies. This effect is automatically taken into consideration if we apply Maxwell's equations of electromagnetic fields ; however, it is better to derive a simple model for the simplicity of analysis.

Acknowledgments

This study was supported by Yasukawa Electric MFG. Co., Ltd. and by a Grant-in-Aid for Scientific Research (C) from The Japan Ministry of Education, Science and Culture, No. 6355 0191. The authors also thank Mr. S. Fujino for his help in preparing the setup of the thrust bearing.

References

(1) Matsumura, F., Kobayashi, H. and Akiyama, Y., Fundamental Equation of Horizontal Shaft Magnetic Bearing and Its Control System Design, Trans. Inst. Elect. Eng. Japan, (in Japanese), Vol. 101, No. 6, C (1981), p. 137.

(2) Matsumura, F., Tanaka, Y., Kido, M. and Akiyama, Y., Composition of Horizontal Shaft Controlled Magnetic Bearing System and Its Experimental Results, Trans. Inst. Elect. Eng. Japan, (in Japanese), Vol. 103, No. 9, C (1983), p. 209.

(3) Fukata, S., Kouya, Y. and Tamura, H., Dynamics of Active Magnetic Bearings, Trans. Jpn. Soc. Mech. Eng., (in Japanese), Vol. 53, No. 490, C (1987), p. 1201.

(4) Fukata, S., Kouya, Y., Tamura, H. and Miyashita, N., Experimental Study of Active Magnetic Bearing, Proc. ICMD, Shenyang, China, (1987), p. 130.

(5) Inami, S. and Hisatani, M., Dynamic Characteristic Simulation of Active Magnetic Bearings, Trans. Jpn. Soc. Mech. Eng., (in Japanese), Vol. 54, No. 508, C (1988), p. 3015.

(6) Watanabe, T., Okino, K. and Sasaki, S., A New Control Law for Magnetic Bearings, Trans. Jpn. Soc. Mech. Eng., (in Japanese), Vol. 36, No. 284 (1970), p. 578.

(7) Engelmann, R. H., Static and Rotating Electromagnetic Devices, Marcel Dekker, Inc., New York, (1982).